Wind Engineering Joint Usage/Research Center
FY2022 Research Result Report

Research Field:
Research Year: FY2022
Research Number: 22222009
Research Theme: Evaluation of ventilation performance and effective effectiveness of devices in actual block area

Representative Researcher: Takashi Kurabuchi (Tokyo University of Science)

Budget [FY2022]: 450,000Yen

*There is no limitation of the number of pages of this report.
*Figures can be included to the report and they can also be colored.
*Submitted reports will be uploaded to the JURC Homepage.

No.1 Study on the ventilation and improvement of thermal environment using buoyant driven ventilation with a single opening

1. Research Aim

The 2003 revision of the Building Standard Law stipulated regulations for the installation of mechanical ventilation equipment with a certain number of ventilation cycles (so-called 24-hour ventilation equipment, etc.) to prevent indoor contamination by substances that may cause sanitary problems in living rooms, as a measure against sick house syndrome. In addition to this, recently, active ventilation of living rooms is required to prevent the transmission of new coronaviruses.

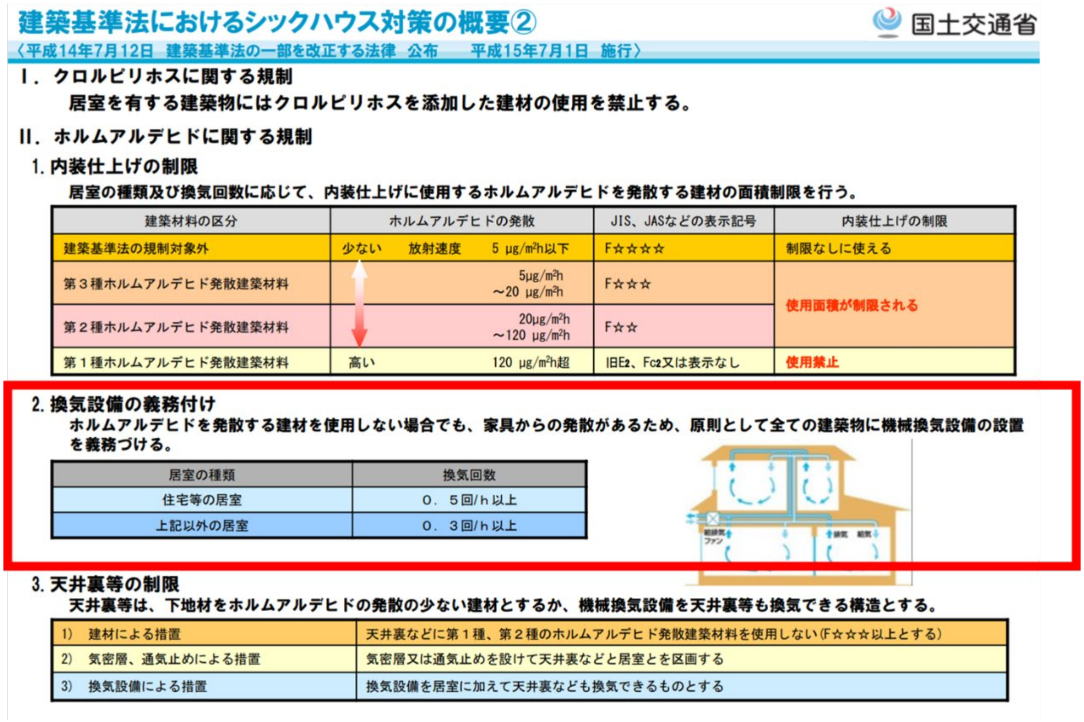

建築基準法におけるシックハウス対策の概要②

国土交通省

〈平成14年7月12日 建築基準法の一部を改正する法律 公布 平成15年7月1日 施行〉

I. クロルピリホスに関する規制

居室を有する建築物にはクロルピリホスを添加した建材の使用を禁止する。

II. ホルムアルデヒドに関する規制

1. 内装仕上げの制限

居室の種類及び換気回数に応じて、内装仕上げに使用するホルムアルデヒドを発散する建材の面積制限を行う。

建築材料の区分	ホルムアルデヒドの発散	JIS、JASなどの表示記号	内装仕上げの制限
建築基準法の規制対象外	少ない 放射速度 5 μg/m²h以下	F☆☆☆☆	制限なしに使える
第３種ホルムアルデヒド発散建築材料	5μg/m²h ～20 μg/m²h	F☆☆☆	使用面積が制限される
第２種ホルムアルデヒド発散建築材料	20μg/m²h ～120 μg/m²h	F☆☆	
第１種ホルムアルデヒド発散建築材料	高い 120 μg/m²h超	旧E2、Fc2又は表示なし	使用禁止

2. 換気設備の義務付け

ホルムアルデヒドを発散する建材を使用しない場合でも、家具からの発散があるため、原則として全ての建築物に機械換気設備の設置を義務づける。

居室の種類	換気回数
住宅等の居室	０．５回/ｈ以上
上記以外の居室	０．３回/ｈ以上

3. 天井裏等の制限

天井裏等は、下地材をホルムアルデヒドの発散の少ない建材とするか、機械換気設備を天井裏等も換気できる構造とする。

1) 建材による措置	天井裏などに第１種、第２種のホルムアルデヒド発散建築材料を使用しない(F☆☆☆以上とする)
2) 気密層、通気止めによる措置	気密層又は通気止めを設けて天井裏などと居室とを区画する
3) 換気設備による措置	換気設備を居室に加えて天井裏なども換気できるものとする

Reference: Ministry of Land, Infrastructure, Transport and Tourism, Housing Bureau : Collection of Examples of Efforts to Promote Efficient Ventilation in Buildings
2022/June

Fig.1 Revision of the Building Standards Act

However, many houses built before 2003 are not equipped with mechanical ventilation systems*1 and must be naturally ventilated by opening windows and other openings. In winter, however, there is concern about the deterioration of the indoor thermal environment due to the direct introduction of outside air into the room. Although it is desirable to open two or more openings for natural ventilation, if two openings are opened consecutively for ventilation during winter, when the temperature difference between inside and outside is large, the ventilation volume may become excessive and the thermal comfort of the room may be compromised. Therefore, we investigated the arrangement of heating heat sources to maintain good indoor air quality and thermal comfort during natural ventilation with a single opening in winter.

2. Research Method

2.1 Field Measurement

The field measurement was conducted in a dwelling unit on the fourth floor of an apartment complex in Atsugi City, Kanagawa Prefecture. Fig 2 shows the plan view of the room to be measured, each measurement point, and an outline of the aperture to be examined. The opening width was always 40 mm. The cases studied are shown in Table 1. In each case, the heat generation shown in Table 1 was performed, and the step-down method experiment using CO_2 as the tracer gas was started when the room temperature stabilized, and the local air age and temperature at each point were measured. A measurement point was also set at 1275 mm above the floor (3/4 of the window height) at the opening, and the CO_2 concentration of the exhaust air was measured. For indoor temperature measurements, thermocouples were installed at positions 100 mm above the floor, 1100 mm above the floor, and 100 mm below the ceiling.

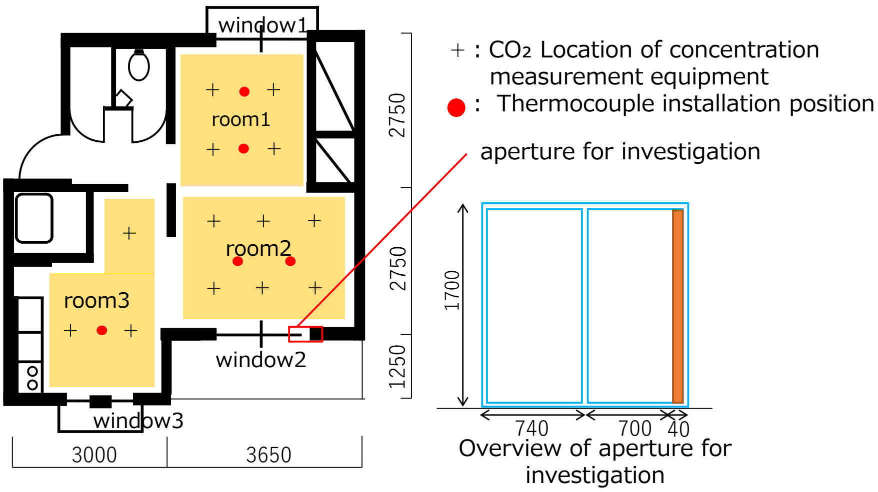

Fig2. overview of the room to be measured

Table1. List of cases to be considered

Case	Heat source location	Calorific value
Case1	Central of each room	Each room 1200W Room2 perimeter zone 1100W
Case2	Room1	Room1 3500W
Case3	Room1	Room1 3500W
case4	room2	Room2 3500W

2.2 CFD Analysis

The analytical model, indoor section model, and CFD analysis summary are shown in Fig 3 and 4 and Table 2. The target outdoor room was subjected to the velocities shown in Table 2 with the +X surface as the inflow boundary condition and a pseudo-no wind condition.

The indoor heating element was modeled as shown in Figure 4, and a heating value of 1200 W or 1100 W was given to the heating surface. The heat transfer coefficient of the wall was assumed to be 7 W/m²-K on the indoor side and 12 W/m²-K on the outdoor side. The heat transfer coefficient values were adjusted from the temperature difference between the wall and the air and the heat transfer rate to set the wall boundary conditions. The thermal transmittance of each part is shown in Table 3. The roof and wall materials were assumed to be concrete, 120 mm thick. From these values, the heat transfer resistance of each section was calculated and given to CFD.

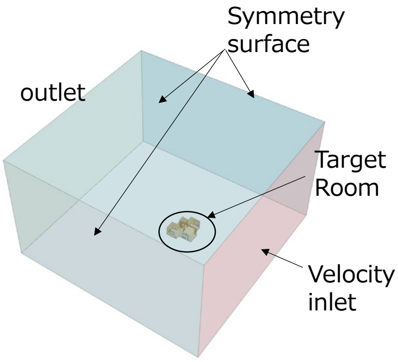

Fig 3. Analysis Model

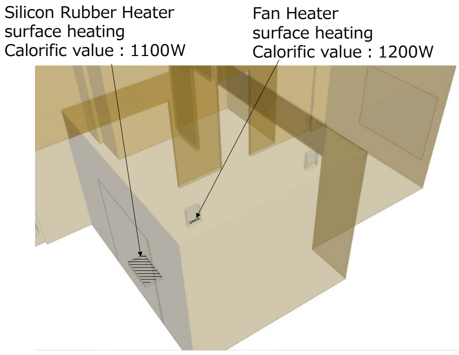

Fig 4. Indoor part model

Table 2. CFD Analysis Overview

Analysis Overview	
turbulence model	Standard k- ε model
Analysis Area	50m(X)×50m(Y)×30m(Z)
Number of meshes	291,974

interior boundary condition	
Heating element	Heat source (1200W, 1200W)
Inside wall	Heat transfer coefficient 6.75 W/(㎡・K)
Outside wall	Heat transfer coefficient 17.25 W/(㎡・K)

outdoor boundary condition	
+X plane	Velocity inlet (-0.1m/s, 0m/s, 0m/s)
-X plan	outlet
+Y plan	Symmetry surface
-Y plan	Symmetry surface
+Z plan	Symmetry surface

Table 3. thermal transmittance

Window name	Thermal transmittance [W/ m²K]
Window 1	2.95
Window 2	6.51
Window 3	3.86

3. Research Result

3.1 Field Measurment Results

Fig 5 shows the measured ventilation frequency in each case and the theoretical value of the ventilation frequency obtained from the difference in indoor and outdoor temperatures. The outdoor air temperature was taken from the AMeDAS data for Ebina, which is closest to the measurement point, and the measured ventilation frequency in each case was the reciprocal of the air age at the exhaust port. The theoretical value of the ventilation frequency obtained from the difference in indoor and outdoor temperatures was calculated from the formula shown in Table 4. The results show that the measured ventilation frequency in case 4 is larger than the theoretical value, but in the other cases, the measured ventilation frequency is generally in line with the theoretical value. This confirms that ventilation by temperature difference is normally performed in this actual measurement. The reason why the ventilation frequency became larger in Case 4 is thought to be due to the fact that the temperature difference between the inside and outside of the opening became larger because the heat source was concentrated in Room 2.

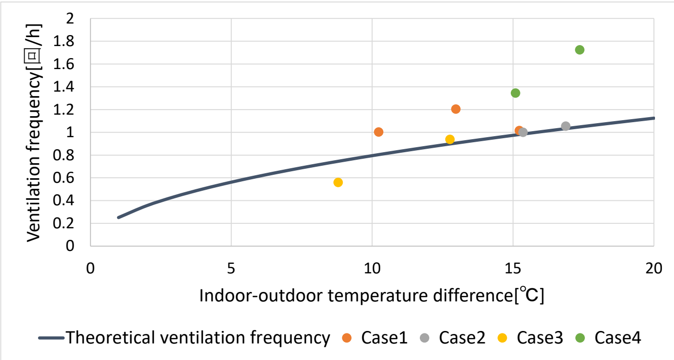

Fig5. Comparison of measured and theoretical ventilation frequency results

Table4. Relation between inside and outside temperature difference and airflow rate

$$Q = \frac{\alpha A}{2\sqrt{2}}\sqrt{\frac{gH\Delta t}{T}}$$

Q : Ventilation volume [m^3/s]
α : Flow coefficient[-]
A : Aperture area[m^2]
g : Acceleration of gravity[m/s^2]
H : Aperture height[m]
Δt : Indoor-outdoor temperature difference[K]
T : Outdoor temperature[K]

3.1.1 Indoor Temperature Measurement Results

Case1(Fig 6)

The vertical temperature distribution for Case 1 is shown in Fig 7. This result shows that there is not much difference in temperature between each room. It can also be seen that the temperature gradient from 1100 mm above the floor to 100 mm below the ceiling is smaller than the temperature gradient from 100 mm above the floor to 1100 mm above the floor.

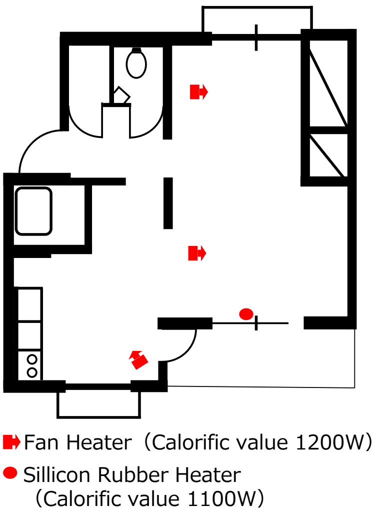

Fig 6. Case1 overview

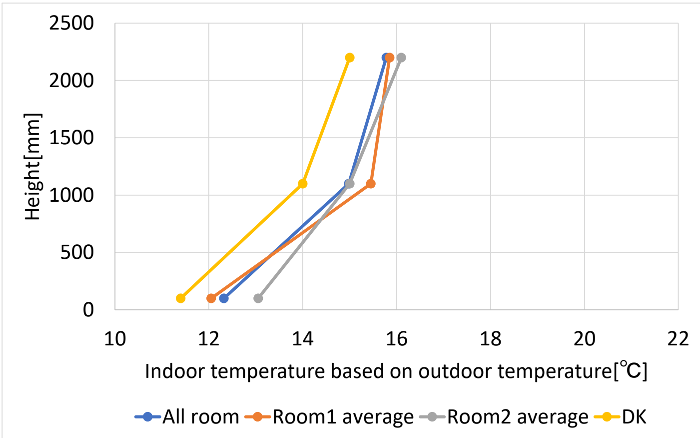

Fig 7. Case1 Vertical temperature distribution（Field measurement）

Case2(Fig 8)

The vertical temperature distribution for Case 2 is shown in Fig 9. The results show that the temperatures in each room are generally equal at the point 100 mm above the floor, but at the points 1100 mm above the floor and 100 mm below the ceiling, the temperatures are higher in the room where the heating elements are installed. The subject dwelling unit has a structure where heat from the heater tends to accumulate near the ceiling due to the hanging walls between rooms, and the amount of heat generated in Room 1 is the largest in Case 2, which is the reason why the temperature near the ceiling in Room 1 is the highest.

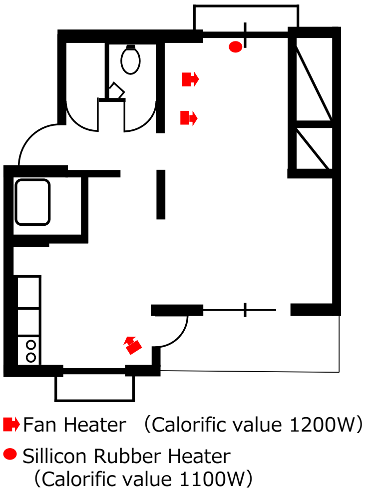

Fig 8. Case2 overview

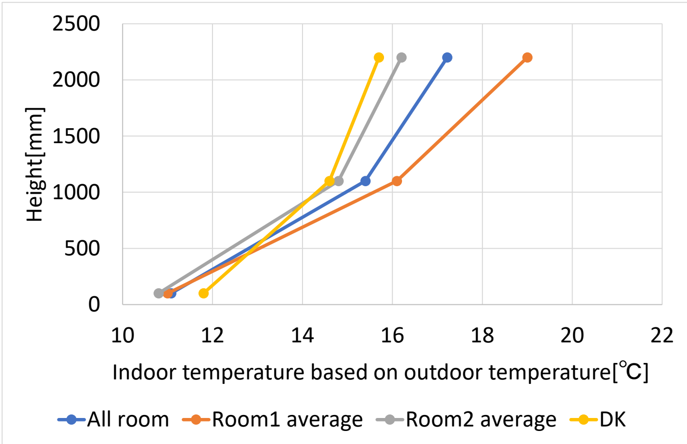

Fig 9. Case2 Vertical temperature distribution (Field measurement)

Case3(Fig 10)

The vertical temperature distribution of Case 3 is shown in Fig 11. The results show that the temperature distribution in each room shows the same trend as in Case 2, but the overall temperature is lower due to the smaller heat generation compared to Case 2. In addition, the temperature gradient from 1100 mm above the floor to 100 mm below the ceiling is smaller than in Case 2, which is thought to be due to the smaller heat generation in Room 2.

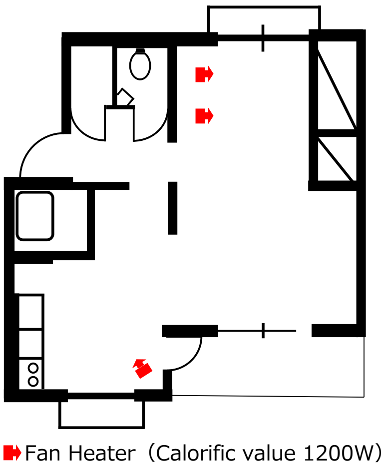

Fig 10. Case3 overview

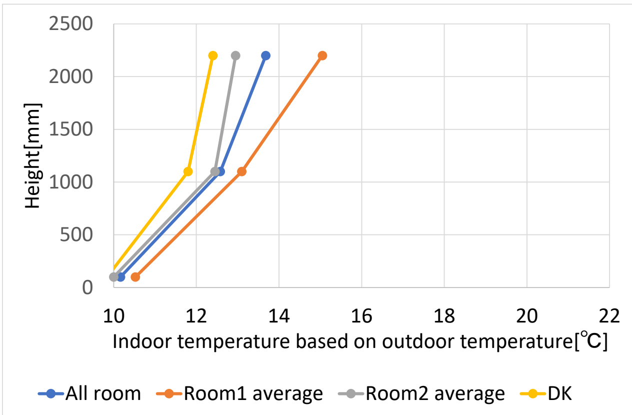

Fig 11. Case3 Vertical temperature distribution (Field measurement)

Case4(Fig 12)

The vertical temperature distribution for Case 4 is shown in Fig 13. The results show that, as in Cases 2 and 3, the temperatures in each room are generally the same at the point 100 mm above the floor, but the temperature in Room 2 is higher at 1100 mm above the floor and 100 mm below the ceiling. As in Case 2, the temperature near the ceiling of Room 2 is considered to be higher in Case 4, where the amount of heat generated in Room 2 is greater, due to the hanging walls between the rooms.

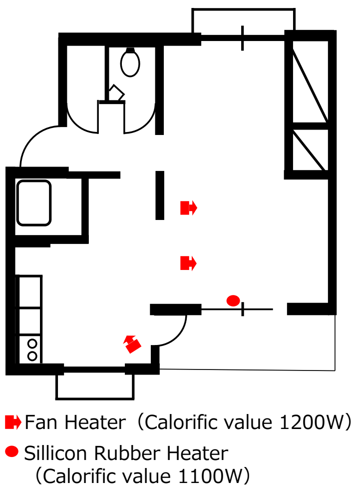

Fig 12. Case4 overview

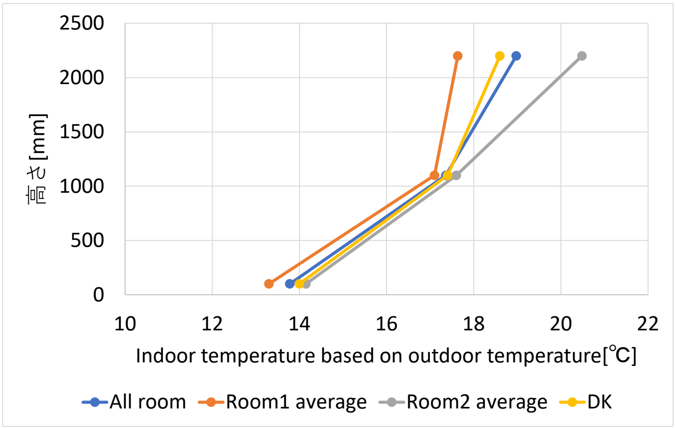

Fig 13. Case4 Vertical temperature distribution（Field measurement）

From the above, it is considered that the ventilation frequency in Case 4 is larger than in the other cases because the temperature difference between the inside and outside of Room 2, which is close to the opening, is larger than in the other cases. The vertical temperature distribution of Room 2 in Case 2 is not significantly different from the vertical temperature distribution in Case 1. This suggests that the amount of ventilation by temperature difference ventilation depends on the indoor/outdoor temperature difference near the opening.

3.1.2 Age of Air Measurement Results

Fig 14-17 show the air age distribution maps for each case. The results show that in all cases the values are relatively high in the southwest part of the DK, but the distribution is not highly skewed for the room as a whole. Although there is a difference when comparing the average air age of the room among the cases, it depends on the ventilation frequency in each case, and there is no difference in the local air age due to the location of the heating elements. Based on the above, temperature difference ventilation is considered to be effective in terms of improving the air quality of the entire room.

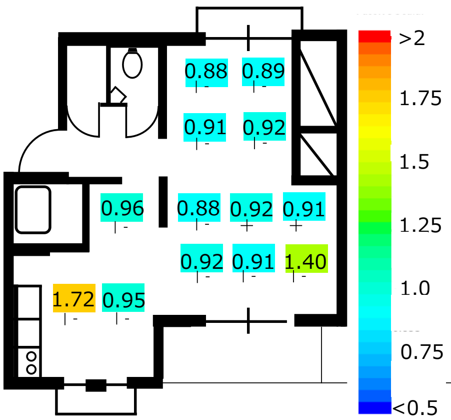

Fig14. Case1 Distribution of Age of Air [h]

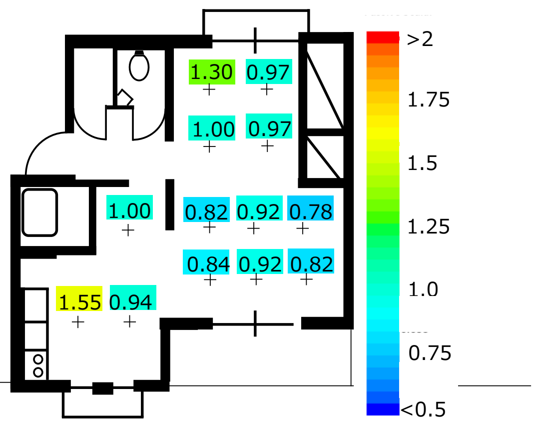

Fig15. Case2 Distribution of Age of Air [h]

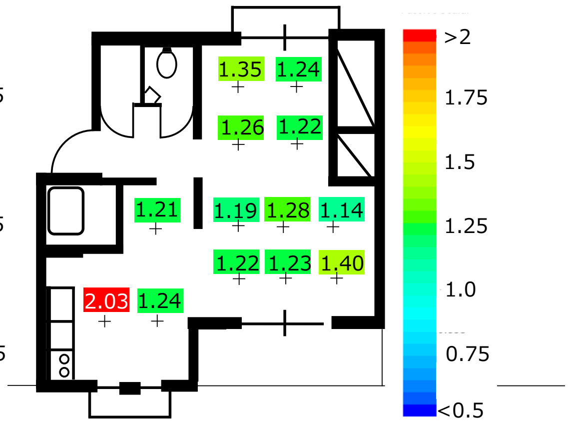

Fig16. Case3 Distribution of Age of Air [h]

Fig17. Case4 Distribution of Age of Air [h]

3.2 CFD Analysis Results

Vertical temperature distributions for each case are shown in Fig 18-20. Although the steady-state analysis was performed in the CFD analysis of this study, it cannot be said that this CFD analysis reproduces the measured results because the influence of heat absorption by the frame is considered to be significant under the actual measurement conditions. However, the vertical temperature distribution in each case is generally similar between the CFD analysis and the actual measurement, so the CFD analysis will be used to study the relationship between the indoor temperature distribution trend and ventilation rate for different heat source locations.

Fig 21 shows the relationship between the indoor/outdoor temperature difference and the ventilation frequency in each case in the CFD analysis results. The theoretical ventilation frequency was calculated using the same formula as in Table 2. The results show that in all cases, the ventilation frequency was calculated close to the theoretical ventilation frequency. In all cases, the CFD analysis value of the ventilation frequency is larger than the theoretical value, especially in case 4. This is consistent with the trend of actual measurements and is thought to be due to the higher temperature near the opening compared to the average temperature of the entire room. From the above, it can be said that the relationship between the indoor/outdoor temperature difference and the ventilation frequency obtained by this CFD analysis is valid.

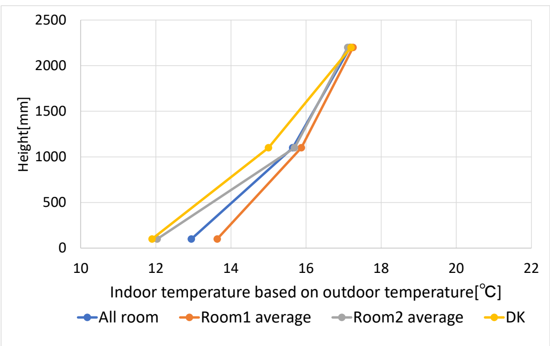

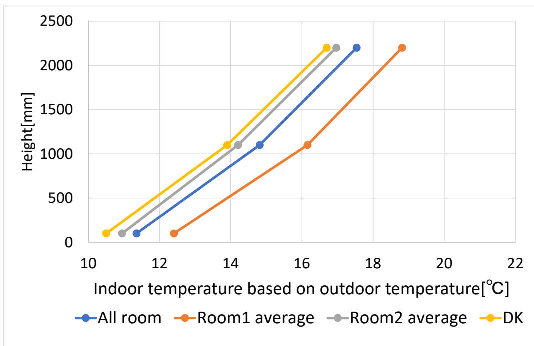

Fig 18. Case1 Vertical temperature distribution（CFD）

Fig 19. Case2 Vertical temperature distribution（CFD）

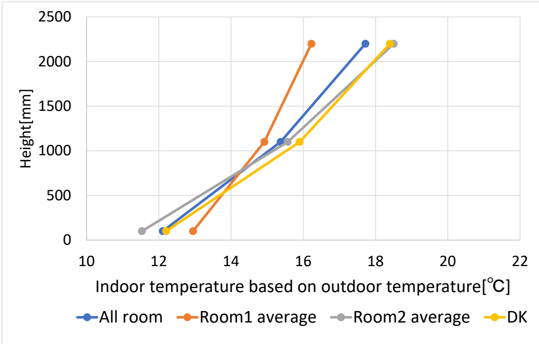

Fig 20. Case4 Vertical temperature distribution（CFD）

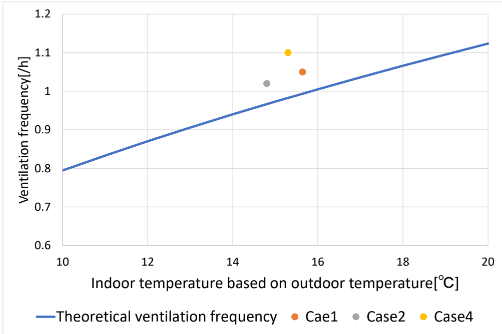

Fig 21. Comparison of ventilation frequency between actual measurement and CFD analysis results

Next, the plane temperature distribution in each case with respect to the outdoor air temperature standard is shown in Fig 22-24. From these results, it can be confirmed that the installation position of the heating elements and the trend of the temperature distribution in each case are consistent. In all cases, low-temperature outside air flows in through the aperture at a height of 100 mm above the floor, and this causes the temperature to decrease near the aperture. This may be the reason for the small temperature of room 2 at 100 mm above the floor in Fig 18-20.

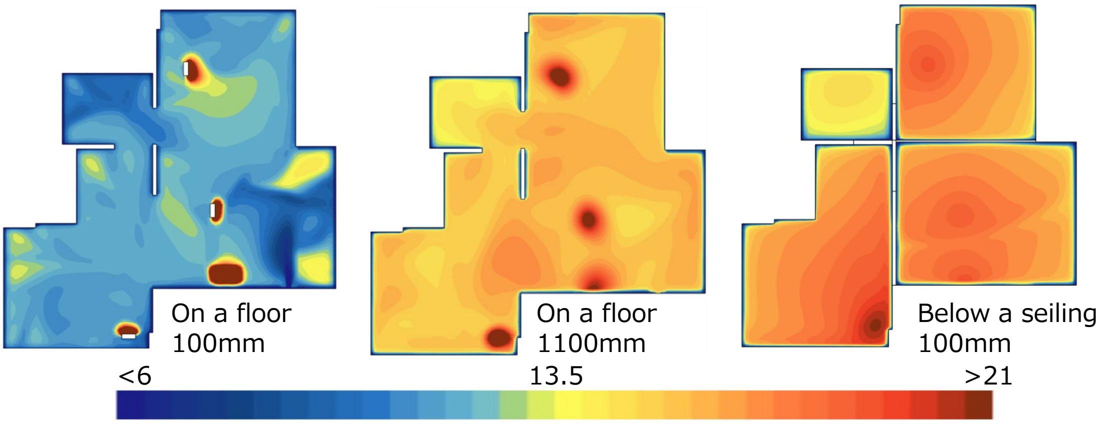

Fig 22. Case1 Plane temperature distribution

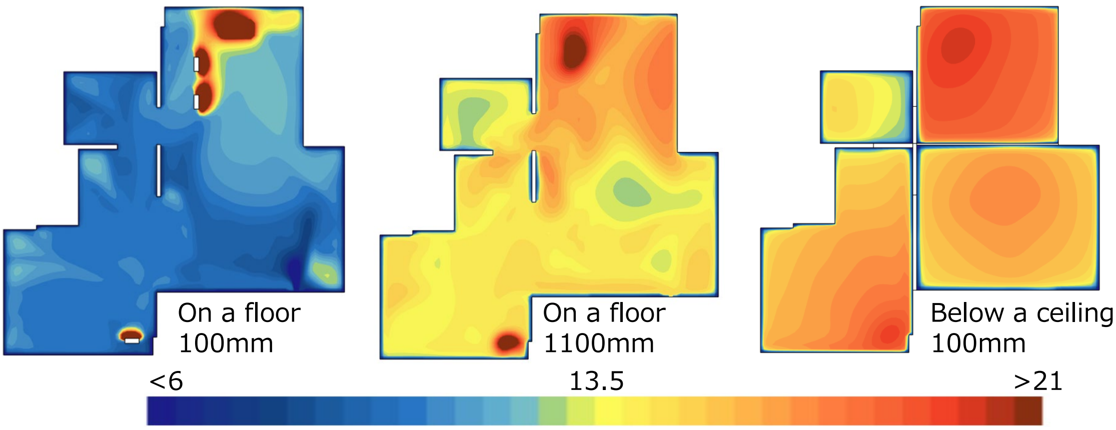

Fig 23. Case2 Plane temperature distribution

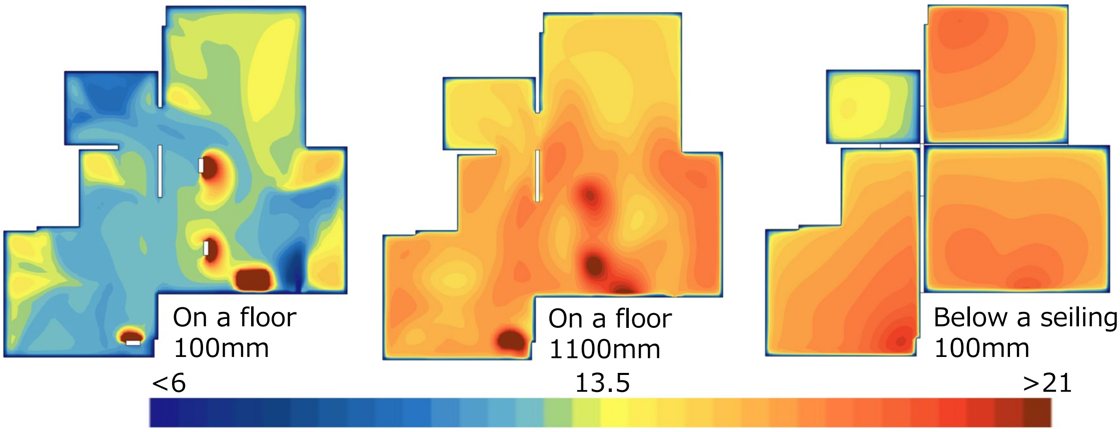

Fig 24. Case4 Plane temperature distribution

3.3 CFD Additional Consideration
3.3.1 Outline of additional consideration

As mentioned in 3.2, there is a high risk of discomfort underfoot due to the inflow of cold outdoor air when ventilating a room using temperature differential ventilation in winter. To remedy this problem, we used CFD analysis to study the effect of installing a heating element at the bottom of the opening to prevent the temperature drop caused by the incoming airflow.

The heaters that had been installed near the opening of room 2 in Case 1 (Fig 6) and Case 4 (Fig 12) were moved to directly below the study opening (Fig 25 and 26) and were modified as Case 1 modified and Case 4 modified, respectively. The CFD analysis conditions were the same as in Chapter 4. The location of the heater after the modification was set on the floor at 100 mm from the opening to the interior.

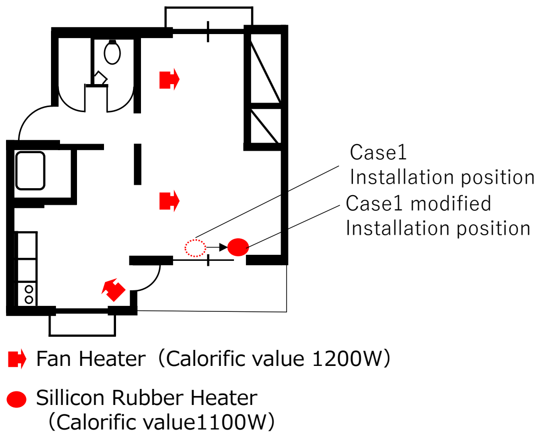

Fig 25. Case1 modified Heating element location

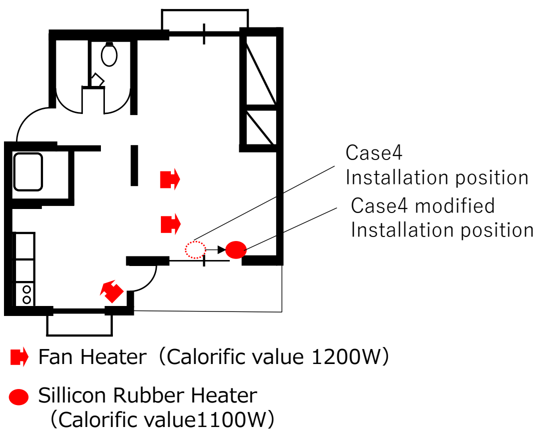

Fig 26. Case4 modified Heating element location

3.3.2 Result of Additional Consideration

Vertical temperature distributions from the CFD analysis results are shown in Fig 27 and 28. Fig 27 shows that there is an overall increase in temperature at 100 mm above the floor, especially in Room 2, with a temperature increase of about 2°C. This indicates that the temperature at 100 mm above the floor has improved and that the temperature difference between the rooms has decreased. Fig 28 also shows that the temperature of Room 2 is smaller than that of Room 1 in Case 4 at 100 mm above the floor, but the relationship is reversed in Case 4. In addition, there is little difference in the temperature distribution in Room 1 between Case 4 and Case 4 modified, but a significant temperature increase is seen in Room 2, especially at 100 mm above the floor. In addition, there is not much difference in temperature distribution between Case 4 and Case 4 modified in Room 2 above 1100 mm above the floor. From the above, it is considered that installing a heating element near the aperture has the effect of preventing the temperature drop at the foot of the floor in the space near the aperture.

Fig 29 shows the results of the comparison of ventilation frequency between Cases 1 and 4 and Cases 1 and 4 modified. Regardless of the position of the heating elements, the ventilation frequency in the additional study slightly increased compared to the existing case, confirming that the heating elements installed near the openings do not hinder ventilation. The increase in ventilation frequency can be attributed to the increase in temperature near the openings, and this trend is consistent with the actual measurements and the results of the CFD analysis in Chapter 5.

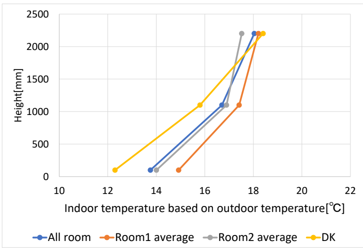

Fig 27. case1 modified Vertical temperature distribution

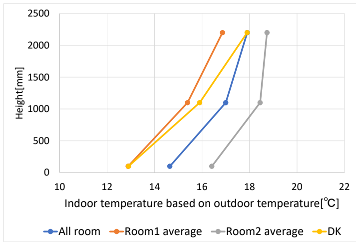

Fig 28. Case4 modified Vertical temperature distribution

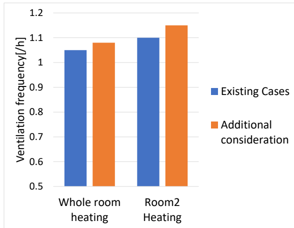

Fig 29. Ventilation frequency comparison

Fig 30 and 31 show the planar temperature distribution maps for each case. These results show that at 100 mm above the floor, the inflow of low-temperature outside air observed in Figures 24 to 26 has been improved. In addition, the overall temperature at 1100 mm above the floor rises compared to Figures 22 and 24, suggesting that the heating elements near the openings contribute to raising the temperature not only near the feet but also in the entire room.

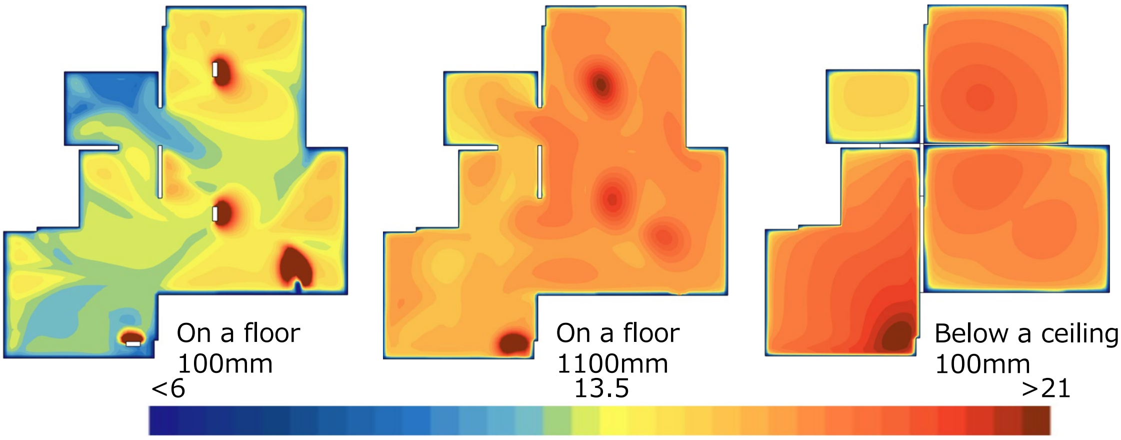

Fig 30. Case1 modified Plane temperature distribution

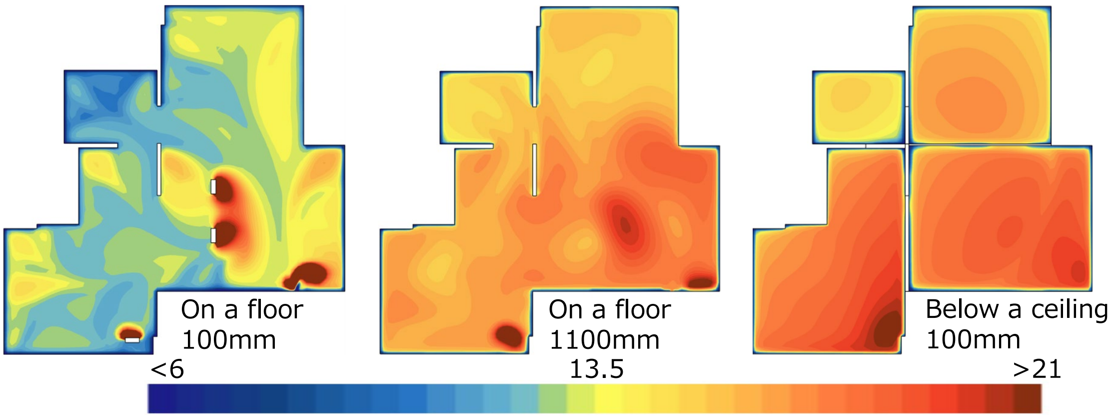

Fig 31. Case4 modified Plane temperature distribution

Table 5 shows the upper/lower temperature difference and unsatisfactory rate in each room based on ISO773*2. In the existing case, the effect of incoming outdoor air caused the vertical temperature difference to increase, especially in Room 2, and the unsatisfactory rate increased accordingly.

Table5. Difference between upper and lower temperatures in each room and unsatisfactory rate and calculation formula

	erature difference between top and bottom			Dissatisfaction rate（%）		
	All room	Room1 average	Room2 average	All room	Room1 average	Room2 average
Case1	2.70	2.24	3.66	3.08	2.10	6.72
Case2	3.46	3.75	3.26	5.74	7.24	4.88
Case4	3.26	1.98	4.04	4.89	1.68	9.07
Case1 modified	2.95	2.49	2.89	3.78	2.60	3.60
Case4 modified	2.36	2.50	2.03	2.32	2.61	1.76

$$PD = \frac{100}{1 + \exp\left(5.76 - 0.856 \cdot \Delta t_{a,v}\right)}$$

PD : Dissatisfaction rate（%）

$\Delta t\_(a,v)$: Temperature difference at 1.1 m above the floor and 0.1 m above the floor（℃）

3.4 Conclusion

The following findings were obtained from this study.

1) The relationship between the indoor/outdoor temperature difference and the ventilation frequency obtained from actual measurements confirmed the validity of indoor ventilation using temperature difference ventilation.

2) The temperature difference between indoor and outdoor temperatures near the opening is considered to be important as the driving force for ventilation.

3) It is considered effective to install a heat source directly below the opening as a measure to improve the deteriorated thermal environment caused by the inflow of cold outdoor air.

Reference

*1 Ministry of Land, Infrastructure, Transport and Tourism, Housing Burea : Collection of Examples of Efforts to Promote Efficient Ventilation in Buildings
2022/June

*2 ISO 7730-2005 Ergonomics of the thermal environment – Analytical determination and interpretation of thermal comfort using calculation of the PMV and PPD indices and local thermal comfort criteria

No.2 Development of Quad-Thermistor for Wind Direction Measurement

1. Research Aim

Hayakawa et al. research*1 aims to improve the reproducibility of exhaust gas properties from gas water heaters in CFD, and requires a detailed understanding of exhaust airflow direction. A split-film probe is often used to measure the wind direction, but it is expensive and difficult to handle because it is prone to breakage. A study*2 by Mizutani et al. suggested the possibility of using two thermal anemometers to measure wind direction. In this study, based on these studies, we investigated a method to measure the exhaust air direction of water heaters in more detail by understanding the wind direction characteristics of a quad thermistor using four anemometers to improve the accuracy of the determination.

2. Research Method

2.1 Wind tunnel test

An overview of the quad thermistor is shown in Fig 1. Four anemometers are placed around the shielding, and the wind direction and speed are identified from the values indicated by each anemometer. The quad thermistors were attached to the traverse in the Eiffel-type wind tunnel apparatus and rotated (Fig 2), and the indicated values of each sensor were obtained at each wind direction angle. The rotation angle in the XY plane shown in Figure 1 is the yaw angle, and the rotation angle in the XZ plane is the pitch angle. Measurements were taken in 15° increments in the range of yaw angle θ = -45 to 45° in five cases with pitch angles φ = -30, -15, 0, 15, and 30°. The scalar wind speed at the installation position of the quad thermistor was used as the reference wind speed.

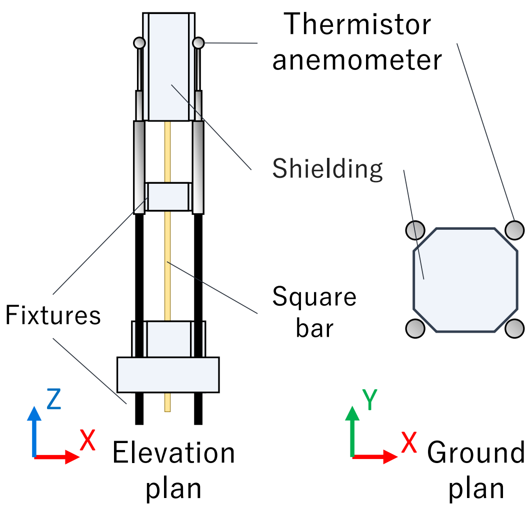

Fig1. Quad-thermistor

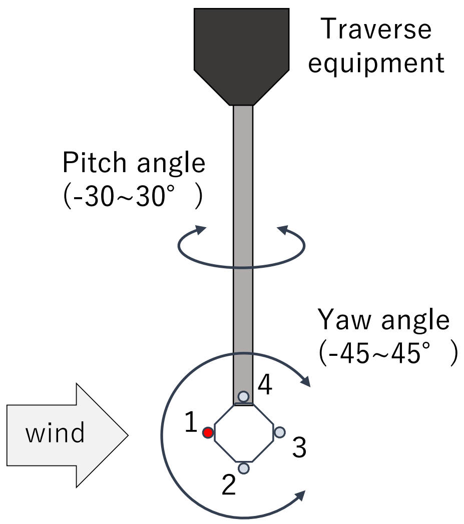

Fig2. Rotation method

2.2 Actual Measurement for Gas Water Heaters

The wind direction angle is determined from the two calculation methods described below by measuring the exhaust air (free jet) from a gas water heater using the quad thermistor created in this study. The square outlet was divided into 9 equal sections (Jet1~9) of 3×3, and measurements were taken at the center of each section at a distance of 100mm and 200mm from the equipment (Fig 3). The quad thermistor is positioned vertically when measuring wind direction in the horizontal (XY) plane and horizontally when measuring wind direction in the vertical (XZ) plane, and is placed so that sensor 1 is aligned with the center of the measurement point (Fig 4). Since the cross-sectional area of the quad thermistor is 4.15% of the total air outlet area, the effect of blocking was judged to be small (Fig 5). In addition, scalar wind velocities were measured for jets 1 to 9 using a thermal sensor of the same type as that used in the quad thermistor.

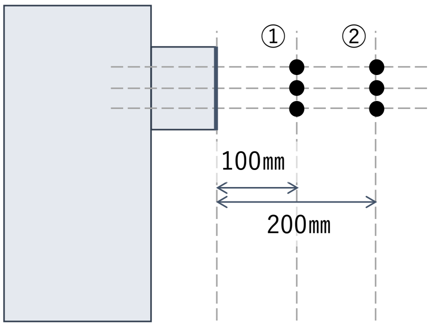

Fig 3. Wind direction measurement point

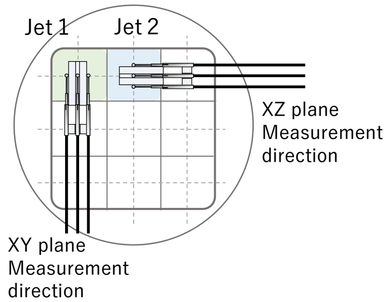

Fig 4. Measuring Method with Quad-Thermistor

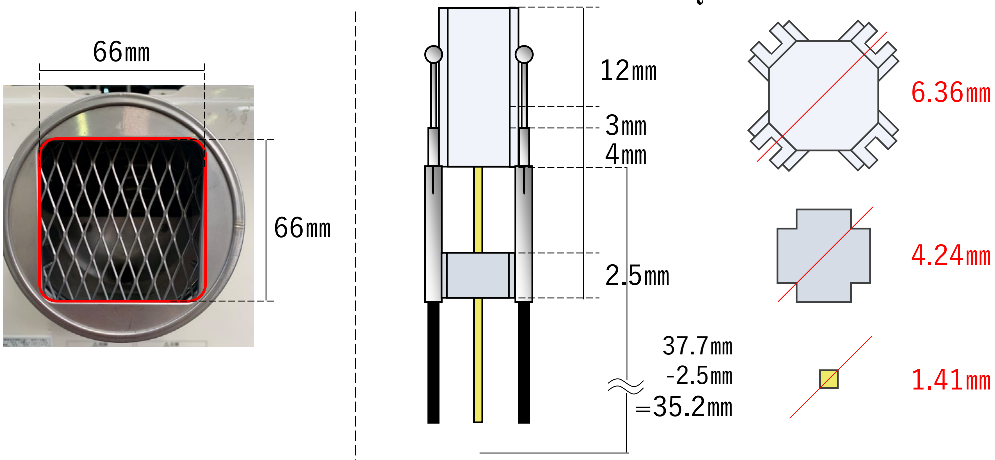

66mm × 66mm = $\underline{4356\text{mm}^2}$

19mm × 6.36mm + 2.5mm × 4.24mm + 35.2mm × 1.41mm = $\underline{181.07\text{mm}^2}$

Fig 5. Consideration of Blocking

3. Research Result

3.1 Measurement Results

The values for each sensor at a pitch angle of 0° are shown in Fig 6. The direction in which sensor 1 faces directly into the wind is 0°, and the values measured in the -45~45° range are used as the 360° wind direction characteristics. Focusing on sensor 1, the lowest values are found in the 150~210° range and the highest values in the 60~90° range. When θ = 0°, which is located on the upwind side, the wind speed decreases due to the effect of stagnation. The pitch angle also affects the wind direction curve (Fig 7), with negative pitch angles tending to have higher values than positive ones in the 45~315° range.

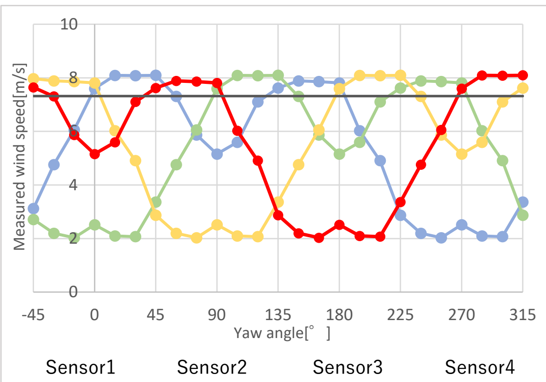

Fig 6. Indicated value of each sensor (0° pitch angle)

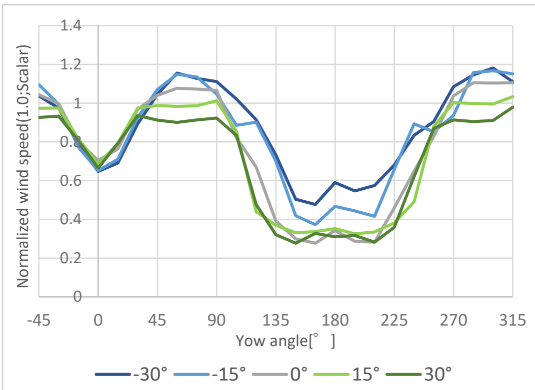

Fig 7. Comparison by pitch angle

3.2 Wind Direction Calculation Method

3.2.1 Calculation Method I

Based on the results of 3.1, a graph approximating the directional characteristics of each sensor as a cos curve is shown in Fig 8. -45°≤θ≤45° and 45°≤θ≤315° can be divided into two sections, which can be approximated by the equation shown in Fig 8 for each section. The approximate equations for sensors 2 to 4 are expressed in the form that the phase of the approximate equation for sensor 1 is shifted by 90°. Equation (2) is used to estimate the wind direction of the object to be measured. Assuming that the wind direction angle of the exhaust air is -45°≤θ≤45°, sensor 1 is within the range of equation (1) and sensors 2~4 are within the range of equation (2), so the three unknowns: a_2, θ, and b_2 of equation (2) can be solved from the three values of 2~4 to determine the wind direction θ.

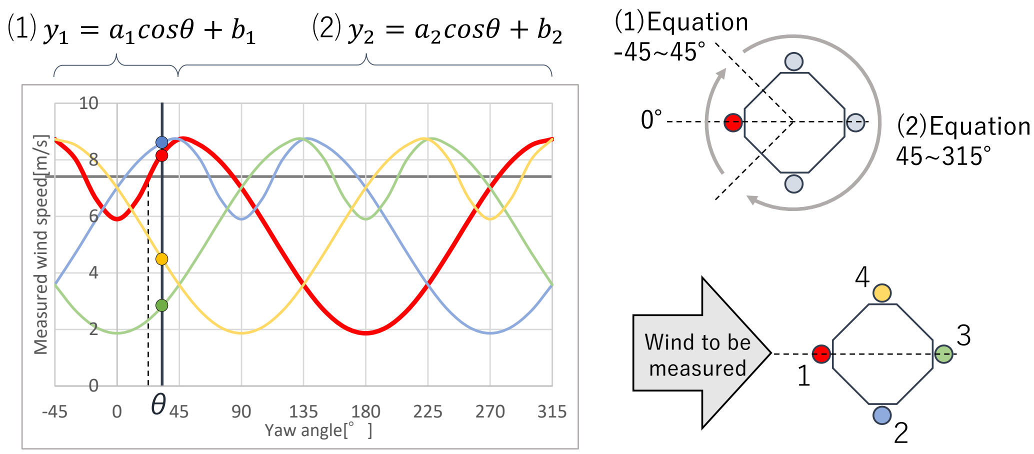

Fig 8.【Calculation Method I】cos curve-fitting

3.2.2 Calculation Method II

In the red frame in Fig 7 (-45°≤θ≤45°), the curve representing the directional characteristics is averaged over all measurement cases and is close to a straight line, so it is approximated by a straight line and expressed as an equation with x as the wind direction angle and y as the reference wind speed (Fig 9). The approximate straight line is classified into four categories: -45°≤θ≤-30°, -30°≤θ≤0°, 0°≤θ≤30°, and 30°≤θ≤45°. The method for determining the wind direction from the values of each sensor is shown in Fig 10. The absolute value of the wind direction is determined from the value of sensor 1, and the sign of the wind direction angle is determined from the relationship between sensor 2 and 4. The sign is positive when 2>4 and negative when 4<2.

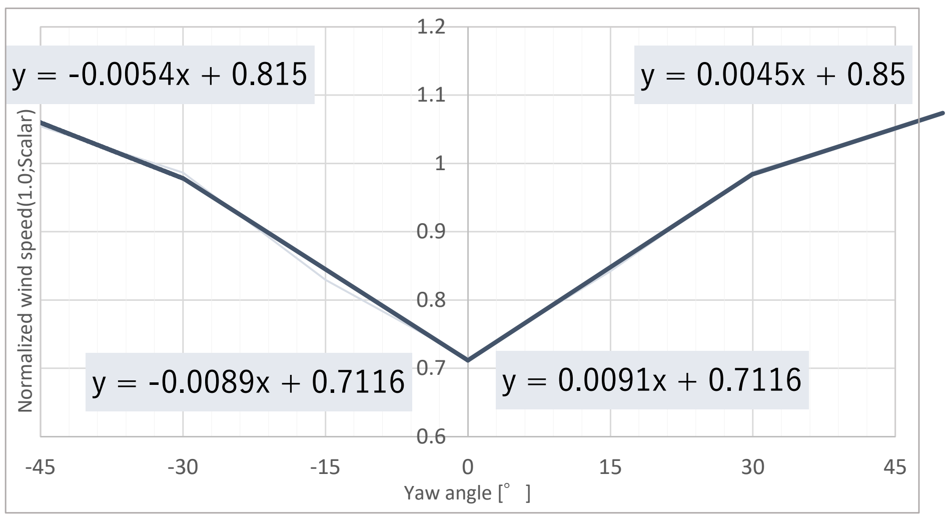

Fig 9.【Calculation Method II】Standardized Approximate Line（-45°≤θ≤45°）

Sensor	Measured wind speed[m/s]	normalization
1	7.27	0.97
2	8.27	1.11
3	5.75	0.77
4	9.77	1.31
Standard wind speed	7.47	1.0

Wind direction is determined by fitting an approximate straight line

Determine the sign from the size of 2 and 4

Fig 10.【Calculation Method II】Method of determining wind direction angle

3.3 Results of actual measurements on gas water heaters

3.3.1 Measured results

From the measurement results of each sensor of the quad thermistor, the wind direction is calculated using the two calculation methods described above. The wind directions determined from calculation methods I and II are shown in Tables 1 and 2, and the two wind directions are referred to as I and II, respectively. Compared to I, II tends to overestimate the wind direction. In the case of II, several measurement points were found to be out of the range of the approximate straight line, such as the yaw angle of jet7 at 100 mm from the device and the pitch angle of jet5.

Comparison with CFD analysis The wind velocity vector distributions in the horizontal plane (Jet4, 5, 6) and in the vertical plane (Jet2, 5, 8) of the middle row of air outlets are shown in Figures 11 and 12, respectively. The wind directions are generally consistent, but in the horizontal plane, the calculated wind direction II for Jet6 and Jet5 shows opposite directions, and in the vertical plane, the wind direction angles are overestimated for Jet2 and 8 in the upper and lower rows.

Table 1. Wind direction determined from Calculation Method I

Jet No.	Horizontality [°]	Vertical [°]	Jet No.	Horizontality [°]	Vertical [°]
1	-16.2	8.2	1	-11.1	11.0
2	-3.9	14.9	2	-3.1	8.0
3	4.4	3.2	3	3.0	6.0
4	-10.0	-6.0	4	-11.3	-7.0
5	0.1	2.4	5	-4.4	-1.6
6	8.9	-1.7	6	1.0	-1.1
7	-17.2	-8.8	7	-0.5	-16.5
8	-3.3	-12.5	8	-3.7	-11.0
9	10.5	-10.4	9	1.9	-11.7

Table 2. Wind direction determined from Calculation Method II

Jet No.	Horizontality [°]	Vertical [°]	Jet No.	Horizontality [°]	Vertical [°]
1	-29.4	28.6	1	-4.1	0
2	-6.3	18.5	2	-3.2	13.2
3	10.6	20.6	3	5.0	13.8
4	-5.6	-2.2	4	-7.2	-13.1
5	25.3	0	5	-11.5	-4.4
6	9.8	-0	6	17.4	-4.6
7	-63.1	-11.9	7	-26.6	-64.3
8	-35.8	-10.2	8	-25.8	-49.0
9	28.1	-8.8	9	33.6	-6.1

3.3.2 Conparison with CFD

Compare the results of the CFD analysis, which generally reproduces the exhaust air from the gas water heater, with the wind directions I and II calculated from the quad thermistor measurements to confirm the accuracy of the calculations. Wind velocity vector distributions in the horizontal plane (Jet4, 5, 6) and in the vertical plane (Jet2, 5, 8) of the middle row of air outlets are shown in Fig 11 and 12, respectively. The wind directions are generally consistent, but in the horizontal plane, the calculated wind direction II for Jet6 and Jet5 shows opposite directions, and in the vertical plane, the wind direction angles are overestimated for Jet2 and 8 in the upper and lower rows.

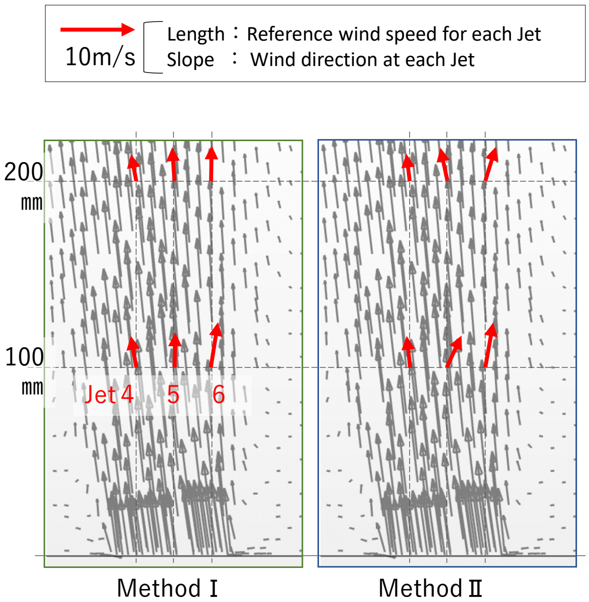

Fig11. Comparison of wind direction (yaw angle)

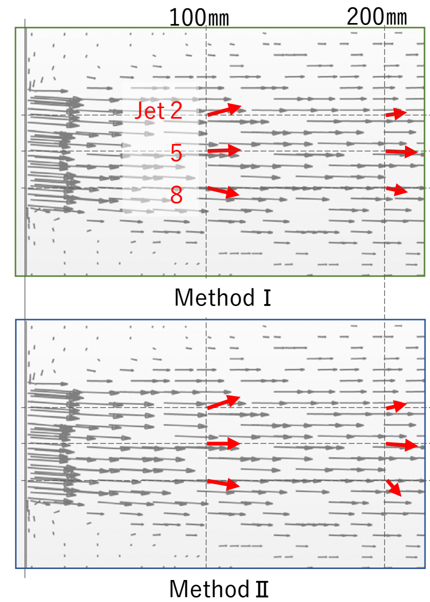

Fig12. Comparison of wind direction (pitch angle)

3.4 Conclusion

The following findings were obtained from this study.

(1) Wind tunnel experiments show that the quad thermistor's wind direction characteristics are as follows: the sensor located near 45° to the wind shows the maximum wind speed, the sensor located downwind shows the minimum wind speed, and the sensor located upwind shows a low wind speed due to stagnation in the direction directly opposite to the wind.

(2) Comparison by pitch angle shows that the wind blowing down has a higher wind speed than the wind blowing up at yaw angles from 45° to 315°.

(3) Comparison of the calculated wind direction from the experiment and the analysis shows that calculation method I, which is an approximation by two large and small cos curves, provides a more accurate wind direction than calculation method II, which is an approximation by a straight line.

Reference

*1 Hayakawa et al : Study on the reproducibility of exhaust gas diffusion from gas water heaters due to the boundary conditions of the outlet [AIJ, 2022]

*2 Mizutani et al : Study on the effect of wind direction fluctuation on natural ventilation and cross ventilation (Part 2) Examination of ventilation measurement method through the window of the experimental model

[A collection of academic lectures at the AIJ, p.1483-1484, 2022.7]

Published Paper etc.
[Underline the representative researcher and collaborate researchers]
[Published papers]
none

[Presentations at academic societies]
1. Akito KONO et al：A study on indoor air quality and thermal comfort under single natural ventilation with single opening [AIJ, 2023]
2. Akito KONO et al：A study on indoor air quality and thermal comfort under single natural ventilation with single opening [SHASE, 2023]
3. Norise TANABE et al：Development of quad thermistor for wind direction measurement [AIJ, 2023]

[Published books]
none

[Other]
Intellectual property rights, Homepage etc.
none

5. Research Group
1. Representative Researcher
Takashi Kurabuchi　Tokyo University of Science / Faculty of Engineering / Professor
2. Collaborate Researchers
1. Kotaro Ishikawa
Tokyo University of Science / Faculty of Engineering / Graduate Student
2. Saki Nakano
Tokyo University of Science / Faculty of Engineering / Graduate Student
3. Mitsuru Takuwa
Tokyo University of Science / Faculty of Engineering / Graduate Student
4. Atsunori Hayakawa
Tokyo University of Science / Faculty of Engineering / Graduate Student
5. Akito Kono
Tokyo University of Science / Faculty of Engineering / Undergraduate
6. Norise Tanabe
Tokyo University of Science / Faculty of Engineering / Undergraduate
7. Toshihiro Nonaka　Tokyo University of Science / Faculty of Engineering / Professor
8. Jeongil Kim
Tokyo University of Science / Faculty of Engineering / Assistant Professor
9 . Kunio Mizutani　Tokyo Polytechnic University/ Faculty of Engineering / Professor

6. Abstract (half page)

Research Theme : Evaluation of ventilation performance and effective effectiveness of devices in actual block area
Representative Researcher (Affiliation) : Takashi Kurabuchi (Tokyo University of Science)

Summary・Figures

STUDY ON THE VENTILATION AND IMPROVEMENT OF THERMAL ENVIRONMENT USING BUOYANT DRIVEN VENTILATION WITH A SINGLE OPENING

In order to obtain sufficient ventilation volume in winter while not compromising thermal comfort, buoyant driven ventilation with a single opening is considered effective.We studied the appropriateness of using it as a ventilation method and the location of appropriate heat sources for improving the thermal environment using actual measurements and CFD analysis, and the following three points were found.

1. We confirmed that buoyant driven ventilation is effective as one of the methods to obtain a stable ventilation rate, based on data obtained from actual measurements.
2. As a driving force for buoyant driven ventilation, temperature differences near the opening are important.
3. As a measure to improve the thermal environment due to the inflow of cold outside air, it is effective to place a heat source directly below the opening.

Development of quad thermistor for wind direction measurement

Hayakawa et al.'s research aims to improve the reproducibility of exhaust gas properties from gas water heaters in CFD, which requires a detailed understanding of exhaust wind direction. A split-film probe is often used to measure wind direction, but it is expensive and difficult to handle due to its tendency to break easily. Mizutani et al. suggested the possibility of using two thermal anemometers to measure wind direction. In this study, we used this as a reference to understand the anemometer characteristics of a quad thermistor using four anemometers to improve the accuracy of determination, and to investigate a method to measure the exhaust air direction of a water heater in more detail. The following findings were obtained from this study: 1.

(1) Wind tunnel experiments show that the quad thermistor's wind direction characteristics are as follows: the sensor located near 45° to the wind shows the maximum wind speed, the sensor located downwind shows the minimum wind speed, and the sensor located upwind shows a low wind speed due to stagnation in the direction directly opposite to the wind.

(2) Comparison by pitch angle shows that the wind blowing down has a higher wind speed than the wind blowing up at yaw angles from 45° to 315°.

(3) Comparison of the calculated wind direction based on the experimental measurements and the analysis shows that the calculation method I, which approximates the wind direction by two large and two small cos curves, is more accurate than the calculation method II, which approximates the wind direction by a straight line.